







Optics Letters

Frequency-doubled Q-switched 4×4 multicore fiber laser system

CHRISTOPHER ALESHIRE,^{1,*}  TIMO EICHNER,^{2,3}  ALBRECHT STEINKOPFF,¹ ARNO KLENKE,^{1,4,5}  CESAR JAUREGUI,¹  GUIDO PALMER,³ STEFAN KUHN,⁶ JOHANNES NOLD,⁶ NICOLETTA HAARLAMMERT,⁶ WIM P. LEEMANS,³ THOMAS SCHREIBER,⁶  ANDREAS R. MAIER,³  AND JENS LIMPERT^{1,4,5,6}

¹Institute of Applied Physics, Abbe Center of Photonics, Friedrich Schiller University Jena, Albert-Einstein-Str. 15, 07745 Jena, Germany

²Center for Free-Electron Laser Science and Department of Physics Universität Hamburg, Luruper Chaussee 149, 22761 Hamburg, Germany

³Deutsches Elektronen Synchrotron (DESY), Notkestraße 85, 22607 Hamburg, Germany

⁴Helmholtz-Institute Jena, Fröbelstieg 3, 07743 Jena, Germany

⁵GSI Helmholtzzentrum für Schwerionenforschung, Planckstraße 1, 64291 Darmstadt, Germany

⁶Fraunhofer Institute for Applied Optics and Precision Engineering, Albert-Einstein-Str. 7, 07745 Jena, Germany

*christopher.aleshire@uni-jena.de

Received 8 February 2023; revised 22 March 2023; accepted 24 March 2023; posted 24 March 2023; published 14 April 2023

Frequency doubling of a Q-switched Yb-doped rod-type 4×4 multicore fiber (MCF) laser system is reported. A second harmonic generation (SHG) efficiency of up to 52% was achieved with type I non-critically phase-matched lithium triborate (LBO), with a total SHG pulse energy of up to 17 mJ obtained at 1 kHz repetition rate. The dense parallel arrangement of amplifying cores into a shared pump cladding enables a significant increase in the energy capacity of active fibers. The frequency-doubled MCF architecture is compatible with high-repetition-rate and high-average-power operation and may provide an efficient alternative to bulk solid-state systems as pump sources for high-energy titanium-doped sapphire lasers.

© 2023 Optica Publishing Group under the terms of the [Optica Open Access Publishing Agreement](#)

<https://doi.org/10.1364/OL.487334>

The development and scaling of frequency-converted laser systems based on near-infrared fundamental wavelengths has accelerated in recent years due to growing interest in new industrial and scientific applications. Second harmonic generation (SHG) of these sources can be applied to laser machining and materials processing techniques [1,2] and pump source development for next-generation ultrahigh-energy laser systems [3–5]. In the latter category, among the most demanding applications is the development of high-repetition-rate ultrafast sources for laser plasma acceleration (LPA); specifically, next-generation titanium-doped sapphire lasers pumped in the blue-green spectral region [6–8]. A working LPA system based on Ti:sapphire will require multi-joule femtosecond-class drive laser pulses with repetition rates of kHz or greater and unprecedented operating efficiency; green pump sources capable of driving such a system do not currently exist and are thus a topic of ongoing development. Candidate pump sources are typically frequency-doubled 1- μ m lasers based on neodymium or ytterbium in

bulk hosts. Several demonstrations with Yb-doped crystals have achieved joule-class or greater frequency-doubled pulse energies [9–11]. Thermal management in these systems is of critical importance and typically limits the repetition rate to the ~10 Hz range, although at least one system has been operated at 1 kHz through careful distribution of the thermal load over numerous amplification stages [12]. These bulk solid-state systems require extensive vacuum- and cryogenic cooling systems which contribute to a high cost and complexity, a large system footprint, and low overall energy efficiency.

The development of high-energy pulsed 1- μ m systems and subsequent frequency-doubling experiments have predominantly focused on improving the average-power capability of laser architectures which are well established as high-energy pulsed sources, such as slab and thin-disk systems. An alternative approach is to scale the energy limits of a laser architecture which is well suited for high-average-power operation, namely Yb-doped fiber lasers and amplifiers. Commercially available fiber systems commonly provide CW powers beyond 1 kW, and coherent beam combining (CBC) of ultrafast fiber lasers has achieved more than 10 kW of average power [13]. However, the highest published pulse energy of such systems is a relatively low 23 mJ [14]. Improving the pulsed energy capability of fiber lasers is particularly attractive for industrial applications where high pulse repetition rates result in higher process throughput, such as laser shock peening [15] or laser lift-off processing of microelectronics [16]. Although active fibers can produce extremely high gain, the small waveguide cross sections are unfavorable for high pulse energies. Limited scaling of the diffraction-limited extractable energy can be achieved through advanced fiber designs with large mode areas [17] or tapered designs to increase the doped volume while maintaining good beam quality [18]. Further scalability can be realized by integrating many doped cores into a single multicore fiber (MCF). Recent CBC experiments with rod-type MCFs have demonstrated this capability with 16 cores in a shared pump

cladding [19]. The MCF CBC architecture has an advantage over equivalent systems of single-core fibers, as the cores are inherently arranged into a dense array without the need for individual beam alignment. While large arrays of independent fibers require many independent subsystems for pumping, cooling, and electrical power, MCFs enable the integration of these systems for more efficient use of energy and laboratory space. In the context of ultrafast CBC, numerical studies predict that a 1-m 10×10 MCF could generate more than 10 kW of average power and 400 mJ pulse energy in a water-cooled system [20]. In this study, the energy limit was a self-imposed “worst-case” scenario dictated by nonlinear effects in stretched ultrafast pulses and not by stored energy in the simulated MCF. The energy scaling potential of MCFs has been experimentally demonstrated using Yb-doped rod-type MCFs with large multimode cores and a tapered geometry which enables mode area scaling [21]. This experiment achieved 49 mJ total energy in 30-ns pulses and is promising not only for CBC, but also for applications which can be driven by high-energy incoherent superposition of laser light. Specifically, large diode arrays are used to pump high-energy solid-state systems [22], and MCF systems with densely integrated arrays of active cores could similarly address this application in spectral regions and operating regimes which are incompatible with diode systems.

The frequency-doubled bulk solid-state systems described above which have been considered for Ti:sapphire pumping generally operate with pulse durations of the order of nanoseconds. For pulsed laser pumping, this is a convenient operating regime, as there is no requirement for chirped pulse amplification, peak power is relatively high for efficient SHG, and pulse generation can be accomplished with modulation of a low-power front end or direct *Q* switching. There are limited demonstrations of ns-class SHG of 1- μ m fiber lasers available in literature. A 2011 experiment using a simple *Q*-switched rod-type fiber laser achieved 48% SHG efficiency with 1-mJ, 13-ns pulses [23]. A more recent demonstration achieved 1-mJ, 35-ns SHG pulses with 70% efficiency using a front-end pulse-shaping system to optimize conversion efficiency [24], although the integration of this functionality required the use of several intermediate amplification stages. At least one example of MCF SHG exists in the literature, based on a 7-core *Q*-switched MCF with coupled cores which achieved a conversion efficiency of 7% and a maximum pulse energy of 17 μ J [25]. In this Letter, frequency doubling of a *Q*-switched oscillator-amplifier system based on a 4×4 Yb-doped tapered MCF is described. These proof-of-concept experiments demonstrate a fiber-based green laser architecture which is natively suitable for efficient high-repetition-rate (kHz or greater) operation. The energy scalability is enhanced by the integration of many parallel waveguides into a single fiber. Additionally, the tapered fiber design scales the waveguide area with improved beam quality and less variation in beam quality among the multimode cores. This feature improves the generation efficiency and the beam quality of the frequency-doubled beams.

A schematic of the rod-type MCF laser system and frequency-doubling stage is shown in Fig. 1. The MCF master-oscillator power-amplifier (MOPA) was a modified version of the system described in Ref. [21], consisting of a *Q*-switched 4×4 MCF oscillator and a tapered MCF amplifier using fibers from the same preform. The amplifier fiber input section was tapered from a 50- μ m core diameter to a 19- μ m core diameter over 20 cm, and the tapered section was used as the amplifier input,

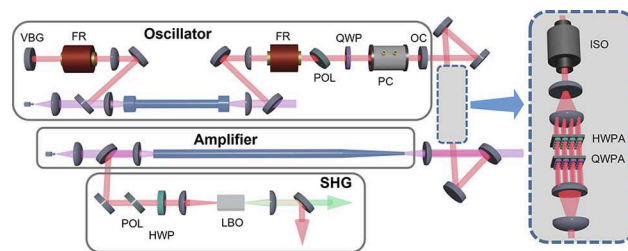


Fig. 1. Schematic of a *Q*-switched MCF oscillator, tapered MCF amplifier, and SHG stage. The inset at right depicts wave plate arrays used for polarization control in the amplifier. VBG: volume Bragg grating mirror, FR: 45-degree Faraday rotator, POL: polarizer, QWP: quarter-wave plate, PC: Pockels cell, OC: output coupler, HWP: half-wave plate, LBO: lithium triborate crystal, ISO: isolator, HWP/QWP: half- and quarter-wave plate arrays, respectively. The 976-nm pump beams, 1030-nm fundamental beams, and 515-nm SHG beams are depicted in violet, red, and green, respectively.

as depicted in Fig. 1. The rest of the fiber maintained a constant 50- μ m core diameter, with a total fiber length of 75 cm, shortened from the original 98-cm length used in Ref. [21] after fiber damage. The oscillator and amplifier were continuously pumped with 976-nm fiber-coupled diodes. For efficient SHG, narrowband operation was accomplished with a reflective volume Bragg grating (VBG) used as a cavity end mirror. The center wavelength of the modified oscillator was 1030 nm with an FWHM bandwidth of 0.5 nm. The amplifier was seeded with pulse energy of 200 μ J/core with a pulse duration of 12 ns.

The MCFs used in these experiments exhibit birefringence which varies between cores and thus require polarization control to achieve uniform output polarization from both the oscillator and amplifier. To compensate for this, the oscillator includes Faraday rotators in the free-space sections [26], producing a linearly polarized oscillator output with uniform powers from the MCF cores and enabling isolation between the oscillator and the amplifier. To produce uniform output polarization of the amplifier for efficient frequency doubling, arrays of half- and quarter-wave plates were inserted between the oscillator and amplifier, with appropriate telescopes for magnification and demagnification of the beam array. By manually adjusting the waveplates during passive transmission of the seed, the total transmission through a thin-film polarizer (TFP) placed after the amplifier fiber could be optimized to 92% (10.6 dB PER), which was maintained during amplification. The reflected s-polarized light contained mostly higher-order fiber modes, as these modes experience different birefringence levels than the fundamental mode.

A $6 \times 6 \times 30$ mm³ LBO crystal was used for SHG after the amplifier. The crystal was cut for type I non-critical phase matching (NCPM) ($\theta = 90^\circ$, $\Phi = 0^\circ$) and heated with a crystal oven to a nominal temperature of 190°C. The calculated spectral acceptance FWHM at 1030 nm for this crystal is 2.3 nm, significantly larger than the MCF system's 0.5 nm bandwidth. The output facet plane of the MCF amplifier was relayed to the crystal and magnified by a factor of 3.75 (imaged core diameter of 188 μ m). In this configuration, the fundamental beams are parallel in the crystal and thus their propagation angles are identical. The angular acceptance bandwidth of type I NCPM in LBO at 1064 nm has been measured at 72 mrad-cm^{1/2} and 99 mrad-cm^{1/2} for the θ and Φ axes, respectively [27]. Assuming similar values

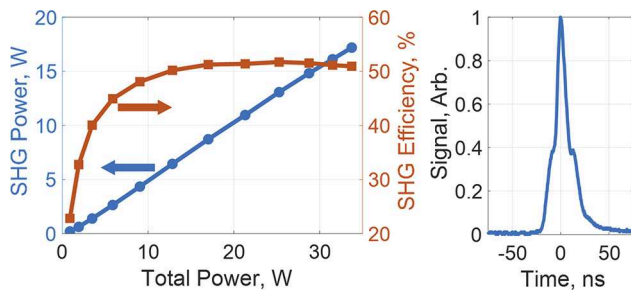


Fig. 2. Left: SHG average power (left axis) and SHG efficiency (right axis) as functions of the combined fundamental and SHG average powers measured after the LBO crystal. Right: oscillator output pulse at 200 μJ per core.

for a 1030-nm wavelength, the FWHM acceptance angles of the 30-mm LBO crystal are 42 mrad and 57 mrad for the θ and φ axes, respectively. Based on the previously measured M^2 values from this fiber amplifier and the implemented magnification, the average beam divergence full angle is approximately 8.5 mrad, significantly lower than the acceptance angles.

The SHG and residual fundamental light were separated directly after the crystal for analysis. The SHG output power and efficiency are plotted in Fig. 2 for a repetition rate of 1 kHz. The low repetition rate was chosen to demonstrate high pulse energy from the amplifier with the available 300-W continuous wave (cw) pump diode, although the MOPA operates with greater efficiency at higher repetition rates, as previously demonstrated in Ref. [21]. Saturation of the SHG efficiency occurred near to 50%, with a maximum measured efficiency of 52% and a maximum SHG average power of 17 W, corresponding to a total SHG pulse energy of 17 mJ. A similar SHG efficiency (48%) from a Q -switched fiber system with similar beam and pulse characteristics was reported in Ref. [23] by Laurila *et al.* The measured SHG spectrum had a 0.5-nm bandwidth, confirming that the 0.5-nm fundamental bandwidth is well within the crystal's spectral acceptance band. At the highest fundamental pulse energies, a slight reduction of the SHG efficiency was observed, which is attributed to the heating of the TFP, resulting in distortion of the imaging within the LBO crystal.

Images of the SHG beam array and its transform plane focused with a 500-mm lens are shown in Fig. 3. Due to the collinear nature of type-I NCPM, there is no walk-off over the length of the crystal and no resultant distortion of the SHG beams (aside from a slightly reduced mode field diameter in comparison to the fundamental, which is typical in SHG with Gaussian beams). The beam quality of each of the sixteen individual beams from this fiber during amplification was previously measured, with

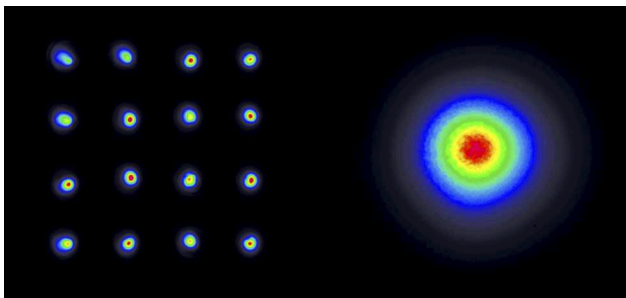


Fig. 3. Images of the SHG beam array (left) and its transform plane (right), where the beams incoherently overlap.

avg. $M^2 \approx 1.5$. The Fourier plane of the SHG array when focused with a single lens had a Gaussian-like shape where all beams were overlapping, as shown in the right-hand side of Fig. 3. It should be noted that in the MCF oscillator depicted in Fig. 1, all cores operate independently, and the amplified beams are not mutually coherent. Thus, the transform plane of the array is an incoherent superposition of nearly Gaussian beams propagating at different angles determined by the focal length of the transform lens and the array dimensions. This is relevant to the considered application of Ti:sapphire pumping, as the incoherent pumping process is dependent on the pump intensity distribution and not on the complex wavefront. The contribution of each beam in the array to the transform-plane intensity distribution is reduced by factor $1/N$, where N is the number of beams. Thus, the effect of this homogenization increases for greater array sizes (more waveguide cores). Note that although a flattop pump profile is typically preferred in high-energy pulsed systems for optimized inversion and thermal profiles, a Gaussian pump and laser profile is desired for efficient coupling to capillary plasma channels in LPA systems [8,28].

These proof-of-concept results are promising for the application of active MCFs as a source of high-energy densely parallelized visible laser light, although numerous improvements can be made to optimize this system. For example, longer fiber lengths and higher seed energies will improve the energy extraction, maximum attainable energy, and overall MOPA efficiency. Operating a pulsed system at repetition rates near the inverse lifetime (~ 1.1 kHz) with cw pump sources is inherently inefficient as significant spontaneous decay will occur between signal pulses. This can be improved with synchronous pulsed pumping to rapidly invert the active material shortly before the arrival of a seed pulse, which is typically done with low-repetition-rate or single-shot systems. In this experiment, the oscillator energy was limited by the onset of parasitic lasing at around 250 μJ per core. With increased pulse energy from the amplifier, the fundamental beams need not be so tightly focused to achieve a high intensity in the SHG crystal, ultimately improving the SHG saturation behavior and conversion efficiency. Common features of the high-energy SHG demonstrations mentioned in the introductory paragraphs are the use of flattop beam shapes and a rectangular pulse shape to homogenize the spatial and temporal intensity and the resulting spatiotemporal SHG efficiency. With these pulse and beam characteristics, conversion efficiencies near to 80% should be achievable [10,12]. Pulse shaping could conceivably be added to the MCF system with appropriate modulation schemes between oscillator and amplifier stages. Flattop/top-hat emission from the cores can potentially be achieved with specialized fiber designs [29–31] integrated into an MCF structure, although this would also modify the Fourier plane intensity distribution. Birefringence compensation using Faraday rotators and polarization control using arrays of waveplates add to the complexity and size of this system. Polarization-maintaining MCF designs are currently under development and would simplify the system architecture and facilitate further scaling. With improved MOPA design and further mode area scaling in a tapered MCF format, an achievable pulse energy of the order of 10 mJ per core is expected. Combined with a further increase in the MCF core count (to a 10×10 array, for example), joule-class fundamental energies could be achieved. When scaled to higher core counts, the MCF pump cladding size can be increased while maintaining a high core-cladding area ratio. This allows the use of high-power,

low-brightness diode pumps which would be incompatible with standard double-clad fibers. A potential challenge associated with scaling the core count is the fabrication of cladding material with a transversally uniform refractive index. To address this, tapered MCFs or techniques for index homogenization may be used [32]. However, as demonstrated above, incoherent combination with many beams is tolerant of nonuniform or imperfect beam quality.

In this Letter, efficient frequency doubling of a high-energy pulsed MCF system has been described, which is potentially applicable to the pumping of high-repetition-rate Ti:sapphire laser systems. Integrating sixteen parallel amplifying waveguides into a multicore fiber enabled compact and efficient energy scaling beyond the energy limits of the cores themselves, and a tapered fiber geometry enabled mode area scaling to multimode core dimensions while maintaining a low output mode order. These MCFs have been initially utilized to demonstrate a new generation of coherently combined laser systems; however, the increased energy capacity of this fiber architecture extends the viability of active fibers to applications where single-core fibers would be unsuitable. As an alternative to bulk solid-state lasers where high-average-power operation provides significant challenges, MCFs and frequency-doubled systems thereof can provide energy-scalable sources compatible with efficient high-repetition-rate operation.

Funding. Fraunhofer-Gesellschaft (Cluster of Excellence "Advanced Photon Sources"); Thüringer Aufbaubank (2018FGR0099); Deutsche Forschungsgemeinschaft (259607349, 416342637); European Research Council (670557, 835306); Bundesministerium für Bildung und Forschung (05K19GUD, 13N15244).

Disclosures. The authors declare no conflicts of interest.

Data availability. Data underlying the results presented in this paper are not publicly available at this time but may be obtained from the authors upon reasonable request.

REFERENCES

1. S. Engler, R. Ramsayer, and R. Poprawe, *Phys. Procedia* **12**, 339 (2011).
2. A. Hess, R. Schuster, A. Heider, R. Weber, and T. Graf, *Phys. Procedia* **12**, 88 (2011).
3. A. Bayramian, J. Armstrong, and G. Beer, *et al.*, *J. Opt. Soc. Am. B* **25**, B57 (2008).
4. H. Yoshida, E. Ishii, R. Kodama, H. Fujita, Y. Kitagawa, Y. Izawa, and T. Yamanaka, *Opt. Lett.* **28**, 257 (2003).
5. S. Gales, K. A. Tanaka, and D. L. Balabanski, *et al.*, *Rep. Prog. Phys.* **81**, 094301 (2018).
6. F. Albert, M. E. Couprie, and A. Debus, *et al.*, *New J. Phys.* **23**, 031101 (2021).
7. K. Nakamura, H.-S. Mao, A. J. Gonsalves, H. Vincenti, D. E. Mittelberger, J. Daniels, A. Magana, C. Toth, and W. P. Leemans, *IEEE J. Quantum Electron.* **53**, 1200121 (2017).
8. "Report of Workshop on Laser Technology for k-BELLA and Beyond," [Online]. Available: https://www2.lbl.gov/LBL-Programs/atap/Report_Workshop_k-BELLA_laser_tech_final.pdf
9. T. Sekine, H. Sakai, Y. Takeuchi, Y. Hatano, T. Kawashima, H. Kan, J. Kawanaka, N. Miyanaga, and T. Norimatsu, *Opt. Express* **21**, 8393 (2013).
10. J. P. Phillips, S. Banerjee, K. Ertel, P. Mason, J. Smith, T. Butcher, M. De Vido, C. Edwards, C. Hernandez-Gomez, and J. Collier, *Opt. Lett.* **45**, 2946 (2020).
11. Z. Hubka, R. Antipenkov, R. Boge, E. Erdman, M. Greco, J. T. Green, M. Horáček, K. Majer, T. Mazanec, P. Mazúrek, J. A. Naylon, J. Novák, V. Šobr, P. Strkula, M. Torun, B. Tykalewicz, P. Bakule, and B. Rus, *Opt. Lett.* **46**, 5655 (2021).
12. H. Chi, Y. Wang, A. Davenport, C. S. Menoni, and J. J. Rocca, *Opt. Lett.* **45**, 6803 (2020).
13. M. Müller, C. Aleshire, A. Klenke, E. Haddad, F. Légaré, A. Tünnermann, and J. Limpert, *Opt. Lett.* **45**, 3083 (2020).
14. H. Stark, J. Buldt, M. Müller, A. Klenke, A. Tünnermann, and J. Limpert, *Opt. Lett.* **44**, 5529 (2019).
15. S. R., G. P., R. K. Gupta, R. G., B. Pant, V. Kain, R. Kaul, and K. S. Bindra, *Lasers Manuf. Mater. Process.* **6**, 424 (2019).
16. R. Delmdahl, R. Pätz, and J. Brune, *Phys. Procedia* **41**, 241 (2013).
17. F. Stutzki, F. Jansen, A. Liem, C. Jauregui, J. Limpert, and A. Tünnermann, *Opt. Lett.* **37**, 1073 (2012).
18. J. Kerttula, V. Filippov, Y. Chamorovskii, K. Golant, and O. G. Okhotnikov, *Opt. Express* **18**, 18543 (2010).
19. A. Klenke, A. Steinkopff, C. Aleshire, C. Jauregui, S. Kuhn, J. Nold, C. Hupel, S. Hein, S. Schulze, N. Haarlammert, T. Schreiber, A. Tünnermann, and J. Limpert, *Opt. Lett.* **47**, 345 (2022).
20. A. Steinkopff, C. Jauregui, C. Aleshire, A. Klenke, and J. Limpert, *Opt. Express* **28**, 38093 (2020).
21. C. Aleshire, A. Steinkopff, A. Klenke, C. Jauregui, S. Kuhn, J. Nold, N. Haarlammert, T. Schreiber, and J. Limpert, *Opt. Lett.* **47**, 1725 (2022).
22. C. L. Haefner, A. Bayramian, and S. Betts, *et al.*, in *Research Using Extreme Light: Entering New Frontiers with Petawatt-Class Lasers III* (SPIE, 2017), p. 1024102.
23. M. Laurila, J. Saby, T. T. Alkeskjold, L. Scolari, B. Cocquelin, F. Salin, J. Broeng, and J. Laegsgaard, *Opt. Express* **19**, 10824 (2011).
24. Y.-H. Cha, S.-W. Kim, S.-W. Kim, J.-H. Shin, and J.-M. Kim, *Appl. Opt.* **60**, 1191 (2021).
25. Y. Huo, G. G. King, and P. K. Cheo, *IEEE Photonics Technol. Lett.* **16**, 2224 (2004).
26. I. Moshe and S. Jackel, *Appl. Opt.* **39**, 4313 (2000).
27. T. Ukachi, R. J. Lane, W. R. Bosenberg, and C. L. Tang, *J. Opt. Soc. Am. B* **9**, 1128 (1992).
28. C. Benedetti, C. B. Schroeder, E. Esarey, and W. P. Leemans, *Phys. Plasmas* **19**, 053101 (2012).
29. F. Kong, G. Gu, T. W. Hawkins, J. Parsons, M. Jones, C. Dunn, M. T. Kalichevsky-Dong, K. Wei, B. Samson, and L. Dong, *Opt. Express* **21**, 32371 (2013).
30. C. Valentin, P. Calvet, Y. Quiquempois, G. Bouwmans, L. Bigot, Q. Coulombier, M. Douay, K. Delplace, A. Mussot, and E. Hugonnot, *Opt. Express* **21**, 23250 (2013).
31. C. Jollivet, K. Farley, M. Conroy, J. Abramczyk, S. Belke, F. Becker, and K. Tankala, in *Fiber Lasers XIII: Technology, Systems, and Applications* (SPIE, 2016), pp. 583–590.
32. F. Kong, C. Dunn, J. Parsons, M. T. Kalichevsky-Dong, T. W. Hawkins, M. Jones, and L. Dong, *Opt. Express* **24**, 10295 (2016).